Fluorescence Emissions and Torsional Conformations in π-Conjugated Chains of PolyDCHD-HS

ARTICLE *in* THE JOURNAL OF PHYSICAL CHEMISTRY C · NOVEMBER 2007

Impact Factor: 4.77 · DOI: 10.1021/jp075012m

Fluorescence Emissions and Torsional Conformations in π-Conjugated Chains of PolyDCHD-HS

Gianni Nannucci, Laura Moroni, Cristina Gellini, Riccardo Chelli,† Pier Remigio Salvi,* and Vincenzo Schettino

Dipartimento di Chimica, Università di Firenze, via della Lastruccia 3, 50019 Sesto Fiorentino, Firenze, Italy

Giovanna Dellepiane

Dipartimento di Chimica e Chimica Industriale, Università di Genova, via Dodecaneso 31, 16146 Genova, Italy

Received: June 27, 2007; In Final Form: September 3, 2007

The fluorescence emission of polyDCHD-HS in solution at room and low temperature and as an amorphous film has been investigated. Extended segments along the polymer backbone are responsible for the observed fluorescence spectrum of polyDCHD-HS in benzene solution. Spectra of the polymer in cyclohexane solution and as an amorphous film give evidence of an additional red-shifted fluorescence, assigned to local substructures behaving as emission centers. Model calculations with the TD-DFT theoretical framework on planar and distorted enyne oligomers have allowed correlation of the $S_0 \rightarrow S_1$ transition energies to chain segments with different torsional angles around the C−C≡C−C axis. In the ensuing structural model, benzene molecules interact attractively with carbazolyl side groups of polyDCHD-HS, thus enhancing the chain rigidity. The interaction energy of carbazolyl groups with cyclohexane is smaller than that with benzene. This leads to more folded chains and, plausibly, also to clusters of few chain segments.

I. Introduction

Molecular systems with extended conjugated π-electron density have stimulated great research interest[1−3] as potential candidates in the development of new materials for optical and electronic applications and have been actively probed as components in electroluminescence,[4] data storage,[5] and nonlinear optical devices.[6] Among them, polymers featuring carbon-rich π-conjugated chains, such as polyacetylenes (PA), polydiacetylenes (PDA), and poly(*p*-phenylenevinylenes) (PPV), have been most extensively studied.[7−9]

For these polymers, a structural model has emerged where the chain is allowed to adopt different conformational arrangements depending on the polymer rigidity and on the strength of attractive interactions between segments.[10−13] According to the model, the absorption and emission properties of the polymer depend on the conjugation length of constitutive chromophores via their transition energies and moments. Moreover, these optical processes are associated with the whole polymer in the sense that they are related to the distribution and location along the chain of the individual chromophores.[9,14] Fluorescence is more properly related to local substructures of the conjugated chain.[9] Following the multichromophoric absorption, fast relaxation mechanisms are responsible for the transfer of the excitation energy into closely located fluorescent sites.[15]

In contrast with these conjugated polymers, poly[1,6-bis(3,6-dihexadecyl-*N*-carbazolyl)-2,4-hexadiyne] (polyDCHD-HS; see Figure 1) stands as a peculiar example of conformationally rigid system and as such has received much attention since its synthesis.[16] Blue and red forms of the polymer have been characterized on the basis of optical spectra.[17−20] The exciton peak around 1.95 eV gives evidence of the so-called blue form. This peak shifts to 2.28 eV in the red form. Accordingly,[17−20] the blue and red forms correspond to different π-electron delocalization along the backbone, leading to a high and low effective conjugation length, respectively. As a second point of interest, polyDCHD-HS is highly soluble in common organic solvents due to the insertion of long alkyl substituents in the 3 and 6 positions of the carbazolyl residues, making the solution phase the simplest environment to investigate the correlation

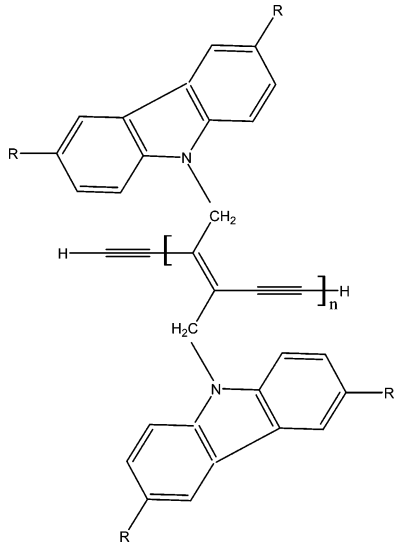

Figure 1. The molecular structure of poly[1,6-bis(3,6-dihexadecyl-*N*-carbazolyl)-2,4-hexadiyne] (polyDCHD-HS), with $R = (CH_2)_{15}CH_3$.

* To whom correspondence should be addressed.

† Also at Laboratorio Europeo di Spettroscopie non Lineari (LENS), Università di Firenze, via N. Carrara 1, 50019 Sesto Fiorentino, Firenze, Italy.

10.1021/jp075012m CCC: $37.00
Published on Web 11/07/2007

between conjugation length and conformational isomerism. In fact, the absorption spectrum depends strikingly on the solvent and shows vibronic structure only when polyDCHD-HS is dissolved in benzene.[18] As to the fluorescence spectrum, to the best of our knowledge, only that in this solvent has been reported.[18,19] In view of the structural information related to the emission properties of polymeric materials,[9] it may be surprising that additional fluorescence studies on condensed phases have not yet appeared. In this paper, we wish to report on the fluorescence of polyDCHD-HS measured in different experimental conditions and with tuning of the excitation wavelength through the visible region from 600 to 470 nm. In fact, by changing the solvent and the temperature or measuring the emission from an amorphous film, several spectral features have been observed and assigned to different conformational structures of the polymer. These results are discussed on the basis of ab initio model calculations relative to planar and twisted oligomers, thus correlating changes in the polyDCHD-HS excitation energies to the different torsional angles around the C−C≡C−C groups. Therefore, we feel that the present analysis of the absorption and fluorescence data may help to characterize in more detail the structure of both the red and blue forms of polyDCHD-HS.

II. Experimental Section

PolyDCHD-HS was synthesized according to the reported procedure[16] and stored in the dark, having noticed that the red/pink solutions in spectroscopic grade benzene and cyclohexane slowly bleach within 5−7 days. Solutions of polyDCHD-HS in these solvents were freshly prepared with elimination of the few undissolved grains by centrifugation. The solution stability was checked during the course of the experiment, for instance, measuring the absorption spectrum at intermediate times and finding no change between the initial and the final spectrum. The solutions were diluted in the range of $10^{-4}-10^{-6}$ (mol of repeat units l^{-1}). The concentration was easily estimated in benzene solutions for which $\epsilon_{534} = 4.3 \times 10^4$ cm^2 (mol of repeat units)$^{-1}$ has been reported.[18] Since the extinction coefficient of polyDCHD-HS in cyclohexane was not known, it was determined at the wavelength of the absorption maximum, that is, 540 nm. From the absorbance of a solution of known concentration, it was found $\epsilon_{540} = 2.0 \times 10^4$ cm^2 (mol of repeat units)$^{-1}$. No evidence of aggregation phases has been reported for benzene concentrations less than 10^{-4} (mol of repeat units l^{-1}).[18] Also in our case, aggregation phenomena have been excluded for polyDCHD-HS in both solvents, having checked that absorption profiles were unchanged for concentrations in the range of $10^{-4}-10^{-6}$ (mol of repeat units l^{-1}). As a second preparation, the amorphous film of polyDCHD-HS was deposited from a toluene solution on a quartz slide under clean room conditions by means of the spin coating technique.[21,22] Spinning velocity was varied between 600 and 6000 rpm. After deposition on the slide, the film was left at room temperature for ≈30 min and then heated at 70 °C for 1 h to evaporate the solvent. The resulting film thickness was about 3 μm. The sample was stored far from light when not used for experiment, and as a result, the absorption spectrum of the film was found to be unaltered with time.

The fluorescence spectra of polyDCHD-HS were measured on a standard Perkin-Elmer spectrophotofluorimeter and with the fluorescence instrumentation assembled in our laboratory. Shortly, the third harmonic of a pulsed Nd:YAG laser operating at a 10 Hz repetition rate was set to pump an optical parametric oscillator (OPO), whose signal output could be tuned in the range of 420−700 nm. To avoid any possible photochemical degradation of the polymer, the beam was not focused on the solution cell nor on the polyDCHD-HS film, and the pulse energy was kept lower than 120 μJ. The fluorescence emission, collected at 90 degrees with respect to the incident beam, was directed on the entrance slit of a double monochromator and sent to a photomultiplier cooled at −10 °C. The fluorescence signal I and the reference signal I_0, this latter obtained by diverting a small fraction of the incident intensity on a photodiode, were processed by a gated integrator and averaged by means of a homemade computer program to give the normalized intensity I/I_0 at each emission wavelength. The spectra measured by means of the two spectrofluorimeters were found to be coincident within the experimental accuracy, with a resolution not better than ≈0.08 eV for the standard and ≈0.003 eV for the laboratory instrument, owing to the narrow excitation bandwidth and to the high dispersion of the double monochromator. Low-temperature fluorescence spectra were measured with the second experimental arrangement, either preparing the solution in a thin quartz cuvette and immerging quickly in liquid nitrogen at 77 K or spraying the solution on the cold finger of a variable temperature cryostat and freezing down to ≈15 K. Finally, fluorescence excitation spectra were obtained at room and low temperature, tuning the excitation wavelength in the range of 600−470 nm at constant excitation intensity.

The absorption spectra of the solution samples and of the film of polyDCHD-HS were measured at room temperature on a Cary 5 spectrophotometer with a spectral resolution of 2 nm (≈0.01 eV at 500 nm).

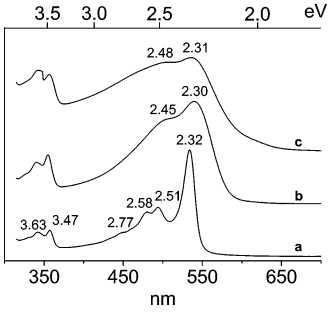

Figure 2. Room-temperature absorption spectra of polyDCHD-HS in benzene and in cyclohexane solution, (a) and (b) traces, respectively, with $c = 2 \times 10^{-5}$ (mol of repeat units l^{-1}), and (c) as a film on a quartz slide. The energies (eV) of the band maxima are indicated. Bands at 3.47 and 3.63 eV are due to the absorption of the carbazolyl residues.

III. Results

A. Absorption Spectra. The absorption spectrum of polyDCHD-HS in diluted benzene solutions has been already reported and discussed[18] as due to polymer chains with negligible interchain interaction. Our room-temperature results, relative to the benzene and cyclohexane 2×10^{-5} (mol of repeat units l^{-1}) solutions and to the film, are collected in Figure 2. In benzene, the polyDCHD-HS spectrum shows well-resolved bands with a remarkably sharp excitonic peak at 2.32 eV with bandwidth $\Gamma_{FWHM} \approx 0.065$ eV, and vibronic additions at 2.51, 2.58, and 2.77 eV. The vibronic peaks at 2.51 and 2.58 eV, 1516 and 2106 cm^{-1} from the origin, have been assigned to conjugated C=C and C≡C stretching modes in the first excited state.[18] They are observed in the ground state at 1519 and 2118 cm^{-1} by FT−Raman spectroscopy,[18] indicating that, upon photoexcitation, conjugated triple bonds of polyDCHD-HS lengthen while double bonds are substantially unaltered. The

TABLE 1: Fitting Parameters for the (b) and (c) Spectra of PolyDCHD-HS in Figure 2[a]

	A_1	A_2	B	C
E_{max}	2.277	2.453	2.638	
Γ_{FWHM}	0.203	0.245	0.459	
E_{max}	2.279	2.460	2.649	2.066
Γ_{FWHM}	0.252	0.280	0.632	0.237

[a] The top two lines are related to the (b) spectrum, and the bottom two lines are related to the (c) spectrum. The three contributions to the observed band profiles, A_1, A_2, and B (see text for details), are centered at E_{max} (eV) with full-width half-maximum, Γ_{FWHM} (eV). A fourth contribution, denoted C, has been considered for the (c) spectrum relative to the film of polyDCHD-HS.

peak at 2.77 eV, 3595 cm^{-1} from the origin, is assigned as a combination of the first two, $1516 + 2106$ cm^{-1}. It is convenient to compare this spectrum with those of other substituted polydiacetylenes such as poly(3BCMU) [where 3BCMU stands for the $(CH_2)_3-OCO-NH-CH_2COO(n\text{-}C_4H_9)$ side group] and polyPTS-12 [where PTS-12 stands for the $(CH_2)_4-O-SO_2$-*p*-toluene side group]. The spectra of poly(3BCMU) in chloroform and of polyPTS-12 in 1,2-dichloroethane are characterized[23] by an extremely broad absorption band, an estimated bandwidth of $\Gamma_{FWHM} \approx 0.57$ eV, centered around 2.64 eV, and with an onset in the spectral range of 2.30−2.34 eV. Absorption profiles of this type have been modeled[14,24] assuming that the polymer has a conformationally disordered structure with chromophores of variable length randomly distributed along the chain. On the contrary, the "molecular" features of the polyDCHD-HS spectrum in benzene suggest that the polymer is composed of extended and well-separated chain segments.[18]

The spectra of polyDCHD-HS in cyclohexane solution and as a film are also reported in Figure 2. We note that the two spectra are similar and more diffuse than that in benzene. The most noticeable difference is the growing absorption intensity on the high-energy side of both spectra with respect to that of the exciton bands, peaked at 2.30 and 2.31 eV. The same was observed for the solution of polyDCHD-HS in chloroform.[18] We attribute the effect to a second absorption process, due to the random portion of polyDCHD-HS present in cyclohexane solution and in the film, overlapping the absorption of chain segments similar to those of the benzene solution. As a consequence, the experimental absorption has been fitted to the sum of two contributions, one due to the exciton origin (A_1) and to vibronic additions (A_2) of the chain segments and the second to the random polymer band (B). The curves have been calculated under the condition that the B maximum is centered around 2.64 eV, as in polyPTS-12 and poly(3BCMU), and has a Γ_{FWHM} bandwidth on the order of that observed for these two polymers. The parameters of the fit are collected in Table 1, while the experimental and calculated data are shown in Figure 3. The bandwidths of the exciton peak A_1 for the polymer in cyclohexane and as a film are 0.20 and 0.25 eV, respectively, in both cases greater than that in benzene. In cyclohexane, broadening arises from less hindered intramolecular motions whose result is to increase the distribution width of the excitation energies. This indicates that the extended portion of the polymer interacts more weakly with this solvent than with benzene. In the solid matrix, the chain segments are in closer contact, thus favoring the occurrence of more disordered yet frozen chain conformations. The observed spectrum of the polyDCHD-HS film shows a shoulder at the absorption onset, slightly above 2 eV (see Figure 2). The fitting curve locates a weak and broad band (C in Figure 3) with maximum at 2.07 eV (see Table 1), suggesting the presence of additional absorbing sites of the polymer at lower energy. In previous papers,[23,25,26] it has been pointed out that during the growth of single polydiacetylene crystals from the monomer, intermediate structural networks are formed as solid solutions of the extended-chain molecules in the lattice of unreacted monomer. In particular, in the case of polyPTS-12, two absorption bands are observed,[23] one at 2.32 eV due to the final polymer and the second at 2.17 eV assigned to the polymer within the crystal of the monomer. Going along with this assignment, we attribute the weak absorption band to segments surrounded by the random polymer portion, being, in this case, totally absent the unreacted monomer. Finally, from Figure 3, it should be noted that the A_1 and A_2 contributions to the absorbance at 2.64 eV (corresponding to a 470 nm wavelength) are much smaller than the B contribution at the same energy and vice versa at 2.30 eV (corresponding to a 540 nm wavelength). This allows a rough estimate of the ratio between the random portion (B) and the extended chains (A) in the polymer using the expression

$$\frac{A_B(470)}{A_A(540)} = \frac{\epsilon_{B,470} c_B}{\epsilon_{A,540} c_A}$$

where $A_B(470)$ and $A_A(540)$ are the absorbances of B at 470 nm and of A at 540 nm, c_B and c_A are the molar concentrations, and $\epsilon_{B,470}$ and $\epsilon_{A,540}$ are the molar extinction coefficients at 470 and 540 nm. We have determined ϵ_{540} of polyDCHD-HS in cyclohexane to be 2×10^4 cm^2 (mol repeat units)$^{-1}$. Instead, $\epsilon_{B,470}$ has been approximated[23] to that of polyPTS-12, $\epsilon_{B,470} = 1.67 \times 10^4$ cm^2 (mol repeat units)$^{-1}$. From the ratio $A_B(470)/A_A(540) = 0.55$ relative to the cyclohexane solution, c_B/c_A is found to be 0.66, indicating that the random polymer in this solution is ≈40%.

B. Fluorescence Spectra. A cursory inspection of the room-temperature fluorescence spectra of Figures 4 and 5 reveals the differences between when polyDCHD-HS is dissolved in benzene and when it is dissolved in cyclohexane. It has been already reported[18] that the fluorescence spectrum of polyDCHD-HS in benzene has almost mirror symmetry and a small Stokes shift with respect to the absorption spectrum. In cyclohexane, the Stokes shift increases from ≈0.034 to ≈0.13 eV, while the spectrum preserves an approximate mirror symmetry. The larger shift in cyclohexane may be explained with the occurrence of local traps to which the excitation energy is channeled,[9] for instance, clusters of extended chains acting as fluorescence sites. The fluorescence spectrum of the film (see Figure 5c) is red-shifted with respect to the absorption spectrum even more largely than that for the cyclohexane solution. In fact, the symmetric and broad fluorescence band ($\Gamma_{FWHM} \approx 0.26$ eV) is centered at 1.95 eV, ≈0.36 eV lower than the absorption maximum. On this basis, we exclude that single extended chains are responsible for the observed fluorescence. Rather, as a reasonable alternative, we point to the formation of emitting centers, where chains collapse into clusters. For polyDCHD-HS in a cyclohexane matrix at low temperature, a broad fluorescence band with a maximum at 2.01 eV is observed, whereas this emission is absent in a benzene matrix under the same experimental conditions (see Figure 6). Comparing the low-temperature excitation and fluorescence spectra of the two solutions reported in Figure 7, we also note that the Stokes shift in benzene solution is smaller (≈0.016 eV) than that at room temperature. In contrast, the shift increases for the other solution, giving rise to a fluorescence band considerably displaced to lower energies but closely resembling the fluorescence band of the film. The smooth variation of the fluorescence emission in this solution

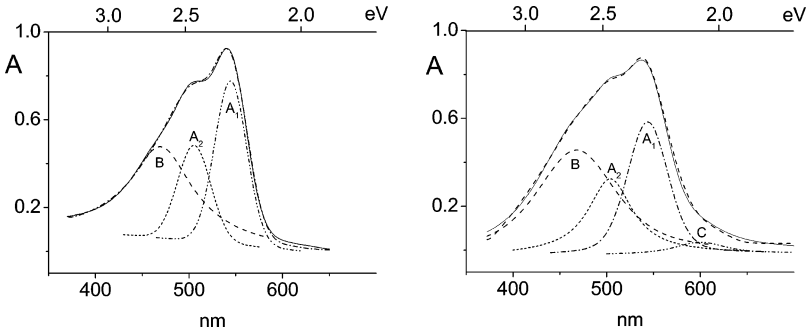

Figure 3. Experimental and calculated intensity of the lowest absorption band of polyDCHD-HS in cyclohexane, left, and as a film, right. The contributing bands to the fitted curves, A_1, A_2, B, and C, are indicated.

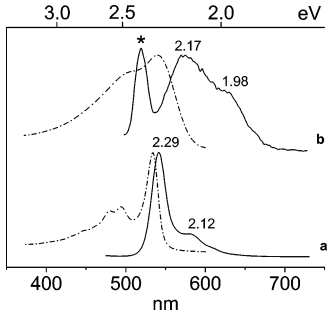

Figure 4. Room-temperature absorption and fluorescence ($\lambda_{exc} = 450$ nm) spectra of polyDCHD-HS solutions 10^{-5} (mol of repeat units l^{-1}) in benzene (a) and cyclohexane (b). The energies (eV) of the fluorescence band maxima are indicated. The asterisk marks the C−H stretching Raman band of cyclohexane.

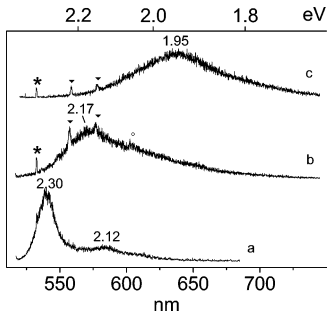

Figure 5. Fluorescence spectra ($\lambda_{exc} = 514$ nm) of polyDCHD-HS in (a) benzene, $c = 2 \times 10^{-5}$ (mol of repeat units l^{-1}), in (b) cyclohexane, $c = 10^{-4}$ (mol of repeat units l^{-1}, and (c) as a film at room temperature. Full triangles, Raman bands of polyDCHD-HS; hollow circles, Raman band of cyclohexane; asterisks, peaks due to stray light from the second harmonic of the Nd:YAG laser. The energies (eV) of the fluorescence band maxima are also indicated.

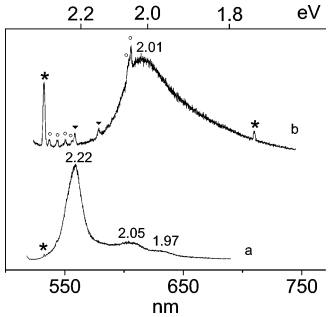

Figure 6. Fluorescence spectra ($\lambda_{exc} = 514$ nm) of polyDCHD-HS in (a) benzene and in (b) cyclohexane, $c = 2 \times 10^{-5}$ (mol of repeat units l^{-1}), at 77 K. Full triangles, Raman bands of polyDCHD-HS; hollow circles, Raman bands of cyclohexane; asterisks, peaks due to stray light from the second and third harmonic, this latter to the second order, of the Nd:YAG laser. The energies (eV) of the fluorescence band maxima are also indicated.

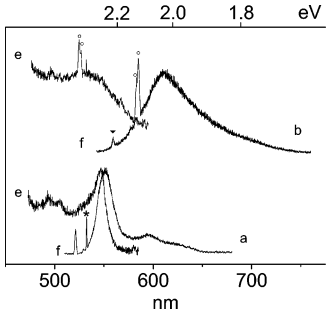

Figure 7. Fluorescence (f, $\lambda_{exc} = 500$ nm) and fluorescence excitation (e, $\lambda_{em} = 600$ and 620 nm for benzene and cyclohexane solutions, traces (a) and (b), respectively) of polyDCHD-HS, $c = 2 \times 10^{-5}$ (mol of repeat units l^{-1}), at 77 K. Full triangle, Raman band of polyDCHD-HS; hollow circle, Raman bands of cyclohexane; asterisk, peak due to stray light from the second harmonic of the Nd:YAG laser; unmarked peak, Raman emission due probably to the quartz enclosure of the sample. The energies (eV) of the fluorescence band maxima are also indicated.

from room to low temperature through the mixed combination of the two spectra up to the cyclohexane crystallization is reported in Figure 8.

Going back to Figure 5b, Raman peaks at 1517 and 2120 cm^{-1} from the exciting line are distinctly observed on the rising background of the fluorescence emission. The dependence of these Raman frequencies on the polymer length has been studied for *t*-butyl-capped enyne oligomers as a function of $1/(P + 1)$, where P is the number of unsaturated bonds.[27] Unsubstituted polyenynes, that is, with an alternating sequence of acetylenic and *trans*-vinylic bonds and with *t*-butyl end groups, *t*Bu−(C≡CCH=CH)$_n$−C≡C-*t*Bu, have been synthesized, and their Raman spectra in hexane solution up to $n = 5$ monomeric units have been measured at room temperature.[27] Therefrom, the stretching frequencies of the conjugated double and triple carbon−carbon bonds for a polymer of infinite length, that is, the intercepts at $1/(P + 1) = 0$, where $P = 2n + 1$, have been found to be[27] 1524 and 2120 cm^{-1}, respectively. The comparison with our frequencies, 1517 and 2120 cm^{-1}, indicates that the extended segments of polyDCHD-HS in cyclohexane are composed of a high number of units. The additional decrease of the observed double bond stretching frequency with respect to the intercept may be ascribed to the inductive, electron-withdrawing effect of the carbazolyl groups. This affects the triple carbon−carbon stretching frequency much less, as the C≡C fragment interacts more weakly with a relatively distant residue.

IV. Discussion

The indications obtained from the analysis of the spectral data on polyDCHD-HS in solution may be summarized as

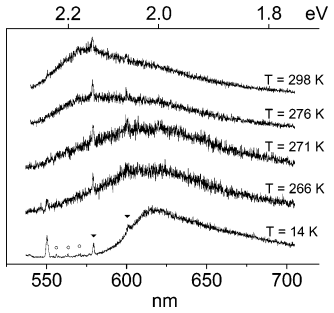

Figure 8. Fluorescence (λ_{exc} = 532 nm) of polyDCHD-HS in cyclohexane, $c = 10^{-4}$ (mol of repeat units l^{-1}), as a function of the temperature down to cyclohexane crystallization. For comparison, the spectrum at 14 K is also shown. Full triangles, Raman bands of polyDCHD-HS; hollow circles, Raman bands of cyclohexane; unmarked peak, Raman emission due probably to the quartz enclosure of the sample.

follows: (1) Well-separated polymer chain segments are found in benzene solution; and (2) on the contrary, several local substructures are responsible for the absorption and fluorescence spectra in cyclohexane. The predominant one is closely related to that occurring in benzene solution. Two others are the random polymer portion and small clusters of chain segments whose emission is red-shifted with respect to the main absorption.

These results invite to a discussion on two major issues concerning the polymer, namely, (i) the dependence of the polymer excitation energies on structural factors and (ii) the sharpness of the polyDCHD-HS spectrum in benzene with respect to that in cyclohexane solution. Starting from the first point, it is useful to recall that the excitation energy E_n of a conjugated polymer may be expressed[23,28,29] as a decreasing function of the number n of monomer units to the E_∞ limit, which represents the excitation energy for $n \rightarrow \infty$. A correct estimate of E_∞ has been proposed in recent years[2,30] using the exponential function

$$E_n = E_\infty + (E_1 - E_\infty)e^{-a(n-1)} \quad (1)$$

where E_1 is the monomer excitation energy and a the saturation rate to E_∞. The relation implying the absorption wavelength, that is, $\lambda_n = \lambda_\infty/[1 + Ae^{-a(n-1)}]$, where $A = (\lambda_\infty - \lambda_1)/\lambda_1$, gives the opportunity to define the effective conjugation length[2] n_{ECL} under the condition $\lambda_\infty - \lambda_{n_{ECL}} \leq 1$ nm

$$n_{ECL} = \frac{\ln[(\lambda_\infty - \lambda_1)\lambda_\infty/\lambda_1]}{a} + 1 \quad (2)$$

It has been found that eq 1 satisfactorily describes the behavior of absorption and fluorescence maxima as a function of n for several groups of conjugated oligomers of various molecular structure.[30] We consider the application of these equations to enyne oligomers, the bare short-chain parents of polyDCHD-HS with *t*-butyl end groups, *t*Bu−(C≡CCH═CH)$_n$−C≡C−*t*Bu. In fact, the absorption spectra of these species, with n = 1, 2, 3, 5, 7, and 9, have been reported for hexane and benzene solutions at room temperature.[27,31] Following early studies,[23,27] we plot in Figure 9 the excitation energies of enyne oligomers as a function of $1/(P + 0.5)$, where P is the number of unsaturated bonds in the oligomer, that is, $P = 2n + 1$, as stated before. According to past observations,[27,31] the dot-dashed line in Figure 9 represents the linear fit of the data. Extrapolating for $P \rightarrow \infty$, that is, $1/(P + 0.5) \rightarrow 0$, a value of $E_\infty \approx 2.25$ eV is obtained.[27,31] It is, however, evident that the experimental data deviate significantly from linearity with increasing P, this behavior being markedly more evident in benzene than in hexane solution. Therefore, as an alternative to the linear plot, we fit the experimental results to eq 1 using the parameters collected in Table 2 (see entries under exp heading). E_∞ values in hexane and benzene are found to be 2.8 and 2.7 eV, respectively. These values are strongly blue-shifted with respect to the lowest transition energies of several polydiacetylene crystals, which are typically below 2.2 eV.[17,32−35] In all of these crystals, the polymer has a planar extended conformation.[26,36−38] For instance, the polyDCHD chain (where DCHD is the DCHD-HS group without the alkyl substituents of the carbazolyl residue) is planar in the crystal,[26] and the exciton peak is observed at 1.91 eV.[17] However, in conjugated polymers, the overall effect of conjugation, $\Delta E = E_1 - E_\infty$, depends not only on the intrinsic confinement of the π-electron density along the chain but also on the torsional motions of contiguous monomer units.[30] Obviously, the second factor lowers the π conjugation and therefore increases E_∞. In our opinion, the large discrepancy between observed peak energies of planar polydiacetylenic chains in the crystal and the limiting E_∞ values of polyenynes in solution, as determined by eq 1, should be attributed to the torsional flexibility of adjacent >C═C< double bond structures around the C−C≡C−C linkage.

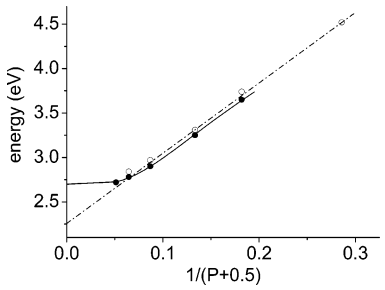

Figure 9. $S_0 \rightarrow S_1$ transition energies (eV) of *t*-butyl-capped enyne oligomers, from n = 2 to 9, in hexane and benzene solution (hollow and full circles, respectively) versus $1/(P + 0.5)$, where P is the number of unsaturated bonds. The dotted-dashed line is the linear fitting to hexane results, and the full line is the exponential fitting to benzene results according to eq 1.

TABLE 2: E_∞Values (eV), Overall Conjugation Energies $E_1 - E_\infty$ (eV), Saturation Rates a, and Effective Conjugation Lengths n_{ECL} of *t*-Butyl-Capped Polyenynes as a Function of the Dihedral Angle τ around the C−C≡C−C Axis[a]

τ	180°	160°	145°	130°	exp	115°
E_∞	1.86	2.00	2.24	2.62	2.70	3.09
$E_1 - E_\infty$	2.55	2.41	2.19	1.75	1.61	1.16
a	0.341	0.362	0.407	0.463	0.525	0.556
n_{ECL}	21	19	16	13	11	10

[a] Results derived from ab initio TD−DFT/B3-LYP/6-31G calculations on oligomers from n = 2 to 9 (see text for details). Planar *trans*-polyenynes correspond to τ = 180°. The entries under the "exp" heading have been evaluated from experimental data of ref 31.

The torsional potential was estimated to be soft in polydiacetylenes, with an energy barrier in the range of 0.5−2 kcal/mol.[39] This value is consistent with our density functional (DF) calculations on the dimer *t*Bu−(C≡CCH═CH)$_2$−C≡C−*t*Bu performed at the B3-LYP/6-31G level.[40] The curve of the minimum potential energy has been determined as a function of the dihedral angle τ ranging from 180 to 0° (trans → cis isomerization), where τ represents the rotation around the central C−C≡C−C group of the two adjacent double bonds. The resulting ab initio energy barrier is 1.9 kcal/mol. In polyenynes longer than the dimer, the barrier is also expected to be low. Substituting the C−C≡C−C group with a single C−C bond,

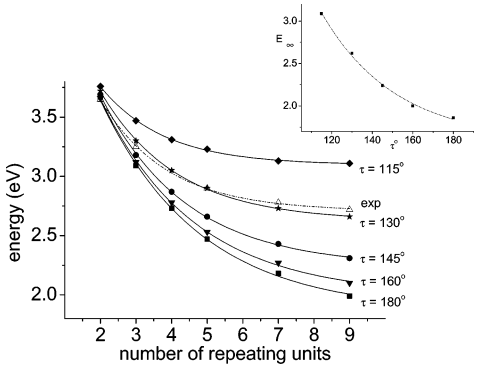

Figure 10. Calculated $S_0 \rightarrow S_1$ transition energies (eV, TD−DFT/B3-LYP/6-31G results) of *t*-butyl-capped enyne oligomers, from $n = 2$ to 9, at a given dihedral angle τ, as indicated. The torsional angle describes the rotation around the C−C≡C−C group of the two adjacent double bonds (see text for details). For the sake of convenience, experimental data from ref 31 are also reported. In the inset, E_∞ values of polyenynes are plotted as a function of the torsional angle τ, from 120 to 180°. Planar *trans*-polyenynes correspond to $\tau = 180°$.

the dyenic molecule *t*Bu−C≡C−CH═CH−CH═CH−C≡C−*t*Bu is obtained, and the energy barrier increases to 10.0 kcal/mol. It is interesting to note that for this system, the central C−C bond elongates from 1.442 Å in the planar ($\tau = 180°$) to 1.482 Å in the perpendicular ($\tau = 90°$) conformation, thus eliminating almost completely the π conjugation between the two ethylenic fragments. In the other case, *t*Bu−(C≡CCH═CH)$_2$−C≡C−*t*Bu, bond lengths of the C−C≡C−C group do not change appreciably as the dihedral angle varies from 180 to 90° due to the fact that two orthogonal π orbitals are available to the triple C≡C bond to preserve the π conjugation.

The effect of torsional flexibility on the transition energies of polyenynes is investigated here with a simple structural model where each monomer unit of the enyne oligomers from $n = 2$ to 9 is allowed to rotate by a constant torsional angle τ with respect to the previous unit. Five τ values, 180, 160, 145, 130, and 115°, have been chosen so that five conformations for each oligomer are considered. (The optimized geometries of all of the conformers are available upon request.) All-trans planar oligomers have $\tau = 180°$ for each monomer unit; all other τ values give rise to partially or totally folded helicoidal conformations. Vertical excitation energies $S_0 \rightarrow S_1$ have been calculated using the Gaussian program[40] with the time-dependent density functional theory (TD-DFT), promoting electrons from the highest occupied MOs to the lowest virtual MOs in a singly excited configuration interaction (SCI) scheme. The set of MOs was chosen according to the following criterion. For example, considering the nonamer in the planar conformation, the SCI calculation includes all 19 π orbitals, the lowest 19 π^* orbitals, and all σ and σ^* orbitals interspersed between those of π and π^* character for a total of 36 occupied and 52 virtual orbitals. The set of MOs for the shorter planar oligomers is composed analogously by 36 occupied and 52 virtual orbitals in order to have an equivalent number of interacting excited configurations. The same set was used for the nonplanar conformations since, in these geometries, all MOs have nonvanishing contributions from the p_z orbitals of carbon atoms due to the disappearance of the molecular plane of symmetry. The calculated vertical excitation energies $S_0 \rightarrow S_1$ are displayed for each torsional angle τ as a function of the number of repeating units, *n*, in Figure 10. For the sake of comparison, the experimental data relative to polyenynes in benzene solution[27,31] are also reported in the figure. By fitting the five series to eq 1, the function $E_\infty(\tau)$ has been determined and plotted in the inset of Figure 10. The E_∞ and n_{ECL} parameters are collected in Table 2. For planar trans ($\tau = 180°$) oligomers, E_∞ amounts to 1.86 eV and n_{ECL} to ≈21. Since the fully extended chains of polydiacetylenic crystals are formed by a number of monomer units not less than n_{ECL}, our value slightly underestimates the observed transition energies, probably due to the neglect of doubly excited configurations stabilizing the ground state. Second, the experimentally determined E_∞ parameter of polyenynes in benzene solution, that is, $E_\infty = 2.7$ eV, is associated with a torsional angle ≤130°, as inferred from the inset of Figure 10. For these oligomers, n_{ECL} is found to be ≈11.

Going from polyenynes to polyDCHD-HS, the *trans*-hydrogen atoms of the ethylenic groups are replaced by the bulky carbazolyl residues with the long alkyl substituents in the 3 and 6 positions (see Figure 1). Ground-state geometries of oligoDCHD, up to the hexamer, have been determined by means of the AM1 semiempirical procedure.[41] Two points of interest are the backbone dihedral angles different from 180° in the optimized structures and the helicoidal arrangement of the carbazolyl residues along the chain, indicating that the hexamer has a relatively compact structure.[41] Our calculation on the tetramer reinforces this conclusion. The equilibrium geometry, obtained from DFT/B3-LYP/6-31G calculations and reported in Figure 11, has the two inner dihedral angles equal to 145°. Due to the large computational burden, it was not possible to deal with a more extended oligomer. Nevertheless, assuming that this dihedral angle is approximately representative of those along the polyDCHD-HS chain, the corresponding E_∞ value in the inset of Figure 10 is ≈2.3 eV, in excellent agreement with the observed exciton peaks of polyDCHD-HS in benzene and cyclohexane solution.

The second point of discussion is the reason why in benzene solution the exciton peak appears sharper than that in cyclohexane. We tried to answer by looking for polymer complexes with the solvent molecules. The $\pi-\pi$ interactions in the benzene dimer have been recently reported.[42,43] Sandwich, T-shaped, and parallel-displaced configurations have been found to be stable, with binding energies on the order of 2 kcal/mol. In our case, the possible occurrence of polymer complexes with benzene and cyclohexane has been probed considering a more simple model, a trimer with carbazolyl residues only on one side with respect to the chain backbone. The DFT/B3-LYP/6-31G calculations show that the two 1:1 complexes have approximately T-shaped configurations, as shown in Figure 12. The binding energies have been calculated, taking into account the basis set superposition error.[44,45] As reported in Table 3, the trimer-benzene complex is more stable than the components by ≈0.5 kcal/mol, while the opposite is true for the trimer-cyclohexane complex. Long-range dispersive interactions have been considered in a second calculation where, after structural optimization at the HF/6-31G level of theory, the MP2 corrections to the Hartree−Fock energies were determined for the complexes and the component units. Both complexes are now stable. The binding energy of the benzene complex is 3 kcal/mol, larger than that of cyclohexane by ≈1 kcal/mol. The important indication here is that the stabilization energy of the trimer-benzene complex with respect to the trimer-cyclohexane complex is ≈1 kcal/mol, irrespective of the level of theory. On this basis, a plausible structure of polyDCHD-HS in benzene is one where chain segments more extended than n_{ECL} have monomer units distorted each with respect to the previous by ≈145° and further stabilized by $\pi-\pi$ interactions of the carbazolyl side groups with benzene. In the case of polyDCHD-HS in cyclohexane, the interaction with the solvent does not lead to a

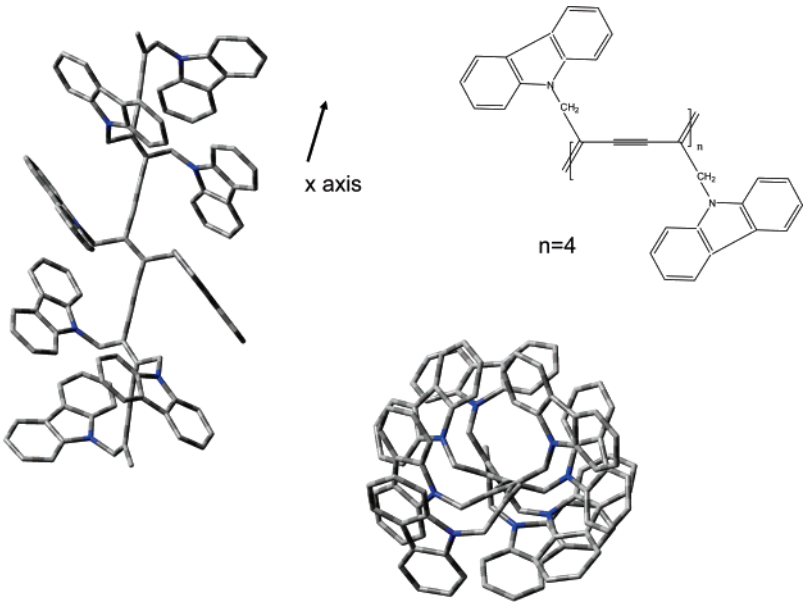

Figure 11. The equilibrium structure of tetraDCHD from DFT/B3-LYP/6-31G calculations, viewed along the *x* and *z* axes. The molecular formula is also sketched on the figure.

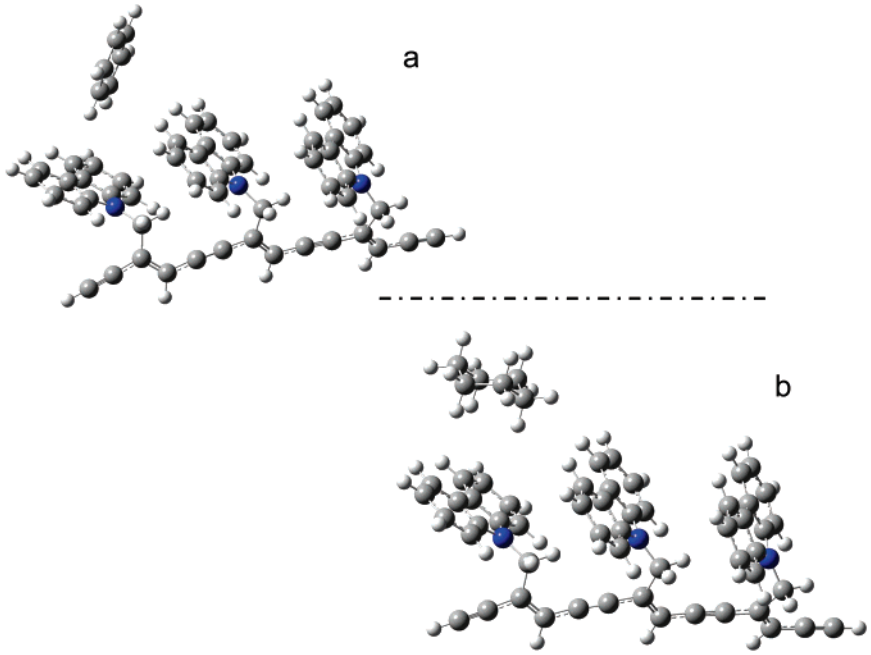

Figure 12. The equilibrium structures of the 1:1 complexes between a model trimer and benzene (top) and between a model trimer and cyclohexane (bottom), according to DFT/B3-LYP/6-31G results.

TABLE 3: Binding Energies (BE, kcal/mol) of the 1:1 Complexes Trimer-Benzene and Trimer-Cyclohexane with Two Different Calculation Methods; the Trimer Structure is Reported in Figure 12

structure optimization	BE calculation	benzene	cyclohexane
DFT/B3-LYP/6-31G	DFT/B3-LYP/6-31G	−0.48	0.50
HF/6-31G	MP2/6-31G	−3.03	−1.93

comparably ordered complex structure. The weakness of long-range attractive interactions between trimer and cyclohexane, if extended to the polymer chain, is the distinctive difference of the cyclohexane with respect to the benzene solution. These indications are consistent with the conclusion that benzene is a good solvent, favoring the polymer to adopt extended conformations where different chain segments result in being well separated by the solvent. On the contrary, cyclohexane is not such a good solvent and forces some chains to collapse into more disordered clusters with segments in closer contact. These latter structures fluoresce at lower energy, behaving as efficient emission centers along the folded polymer.[9]

V. Conclusions

The fluorescence properties of polyDCHD-HS in benzene and cyclohexane solutions and as an amorphous film have been studied under various experimental conditions. Structural information on the polymer conformations in these environments has been obtained. The experimental data have been discussed on the basis of several ab initio calculations. First, the role of torsional flexibility in determining the conformational structures has been emphasized, verifying that the distortion around the acetylenic axis has a low-energy barrier in the unsubstituted dimer, *t*Bu−(C≡CCH═CH)$_2$−C≡C−*t*Bu. Moreover, $S_0 \rightarrow S_1$ excitation energies were determined by means of TD-DFT

calculations for a series of enyne oligomers, $n = 2 \rightarrow 9$, as a function of the torsional angle. Due to attractive $\pi-\pi$ interactions with benzene, the polyDCHD-HS chain stiffens, giving rise to an extended conjugation. A torsional angle of $\approx 145°$ around the C−C≡C−C axis has been estimated between adjacent repeating units. On the contrary, the weaker binding energy between the polymer and cyclohexane allows the formation of chain clusters which are responsible for the observed low-energy fluorescence.

Acknowledgment. The authors gratefully acknowledge Dr. M. Alloisio (University of Genova) for the preparation of polyDCHD-HS films.

References and Notes

(1) Martin, R. E.; Diederich, F. *Angew. Chem., Int. Ed.* **1999**, *38*, 1350−1377.
(2) Meier, H. *Angew. Chem., Int. Ed.* **2005**, *44*, 2482−2506.
(3) Gholami, M.; Tykwinski, R. R. *Chem. Rev.* **2006**, *106*, 4997−5027.
(4) Kraf, A.; Grimsdale, A. C.; Holmes, A. B. *Angew. Chem., Int. Ed.* **1998**, *37*, 403−428.
(5) Feringa, B. L.; Jager, W. F.; de Lange, B. *Tetrahedron* **1993**, *49*, 8267−8310.
(6) Marder, S. R.; Kippelen, B.; Jen, A. K.-Y.; Peyghambarian, H. *Nature* **1997**, *388*, 845−851.
(7) Soos, Z. G.; Galvao, D. S.; Etemad, S. *Adv. Mater.* **1994**, *6*, 280−287.
(8) Yu, J.; Chang, R.; Hsu, J. H.; Fann, W. S.; Liang, K. K.; Hayashi, M.; Lin, S. H. *Trends Phys. Chem.* **1999**, *7*, 77−102.
(9) Barbara, P. F.; Gesquiere, A. J.; Park, S.-J.; Lee, Y. J. *Acc. Chem. Res.* **2005**, *38*, 602−610.
(10) Grosberg, A. Y. *Biophysics* **1979**, *24*, 30−36.
(11) Ivanov, V. A. P.; Binder, K. *J. Chem. Phys.* **1998**, *109*, 5659−5669.
(12) Noguchi, H.; Yoshikawa, K. *J. Chem. Phys.* **1998**, *109*, 5070−5077.
(13) Zhou, Y. Q.; Karplus, M.; Wichert, J. M.; Hall, C. K. *J. Chem. Phys.* **1997**, *107*, 10691−10708.
(14) Kohler, B. E.; Samuel, I. D. W. *J. Chem. Phys.* **1995**, *103*, 6248−6252.
(15) Yu, Z. H.; Barbara, P. F. *J. Phys. Chem. B* **2004**, *108*, 11321−11326.
(16) Gallot, B.; Cravino, A.; Moggio, I.; Comoretto, D.; Cuniberti, C.; Dell'Erba, C.; Dellepiane, G. *Liq. Cryst.* **1999**, *26*, 1437−1444.
(17) Dellepiane, G.; Comoretto, D.; Cuniberti, C. *J. Mol. Struct.* **2000**, *521*, 157−166.
(18) Alloisio, M.; Cravino, A.; Moggio, I.; Comoretto, D.; Bernocco, S.; Cuniberti, C.; Dell'Erba, C.; Dellepiane, G. *J. Chem. Soc., Perkin Trans. 2* **2001**, 146−152.
(19) Alloisio, M.; Moggio, I.; Comoretto, D.; Cuniberti, C.; Dell'Erba, C.; Dellepiane, G. *Synth. Met.* **2001**, *124*, 253−255.
(20) Lanzani, G.; Stagira, S.; Cerullo, G.; Silvestri, S. D.; Comoretto, D.; Moggio, I.; Cuniberti, C.; Musso, G. F.; Dellepiane, G. *Chem. Phys. Lett.* **1999**, *313*, 525−532.
(21) Giorgetti, E.; Margheri, G.; Sottini, S.; Chen, X.; Cravino, A.; Comoretto, D.; Cuniberti, C.; Dell'Erba, C.; Dellepiane, G. *Synth. Met.* **2000**, *115*, 257−260.
(22) Giorgetti, E.; Margheri, G.; Gelli, F.; Sottini, S.; Comoretto, D.; Cravino, A.; Cuniberti, C.; Dell'Erba, C.; Moggio, I.; Dellepiane, G. *Synth. Met.* **2001**, *116*, 129−133.
(23) Wenz, G.; Muller, M. A.; Schmidt, M.; Wegner, G. *Macromolecules* **1984**, *17*, 837−850.
(24) Chang, R.; Fann, J. H. H. W. S.; Liang, K. K.; Chang, C. H.; Hayashi, M.; Yu, J.; Lin, S. H.; Chang, E. C.; Chuang, K. R.; Chen, S. A. *Chem. Phys. Lett.* **2000**, *317*, 142−152.
(25) Enkelmann, V.; Leyrer, R. J.; Wegner, G. *Makromol. Chem.* **1979**, 180, 1787−1795.
(26) Enkelmann, V.; Schleier, R. J. L. G.; Wegner, G. *J. Mater. Sci.* **1980**, *15*, 168−176.
(27) Giesa, R.; Schulz, R. C. *Polym. Int.* **1994**, *33*, 43−60.
(28) Kuhn, H. *J. Chem. Phys.* **1949**, *17*, 1198−1212.
(29) Baughman, R. H.; Chance, R. R. *J. Polym. Sci., Polym. Phys. Ed.* **1976**, *14*, 2037−2045.
(30) Meier, H.; Stalmach, U.; Kolshorn, H. *Acta Polym.* **1997**, *48*, 379−384.
(31) Wudl, F.; Bitler, S. P. *J. Am. Chem. Soc.* **1986**, *108*, 4685−4687.
(32) Bloor, D.; Preston, F. H. *Phys. Status Solidi A* **1976**, *37*, 427−438.
(33) Bloor, D.; Preston, F. H. *Phys. Status Solidi A* **1977**, *39*, 607−614.
(34) Spagnoli, S.; Berrehar, J.; Lapersonne-Meyer, C.; Schott, M. *J. Chem. Phys.* **1994**, *100*, 6195−6202.
(35) Prock, A.; Shand, M. L.; Chance, R. R. *Macromolecules* **1982**, *15*, 238−241.
(36) Kobe, V. D.; Paulus, E. F. *Acta Cryst. B* **1974**, *30*, 232−234.
(37) Enkelmann, V. *Acta Cryst. B* **1977**, *33*, 2842−2846.
(38) Takahashi, Y.; Zakoh, T.; Inoue, K.; Ohnuma, H.; Kotaka, T. *Synth. Met.* **1987**, *18*, 423−426.
(39) Rossi, G.; Chance, R. R.; Silbey, R. *J. Chem. Phys.* **1989**, *90*, 7594−7601.
(40) Frisch, M. J.; Trucks, G. W.; Schlegel, H. B.; Scuseria, G. E.; Robb, M. A.; Cheeseman, J. R.; Montgomery, J. A., Jr.; Vreven, T.; Kudin, K. N.; Burant, J. C.; Millam, J. M.; Iyengar, S. S.; Tomasi, J.; Barone, V.; Mennucci, B.; Cossi, M.; Scalmani, G.; Rega, N.; Petersson, G. A.; Nakatsuji, H.; Hada, M.; Ehara, M.; Toyota, K.; Fukuda, R.; Hasegawa, J.; Ishida, M.; Nakajima, T.; Honda, Y.; Kitao, O.; Nakai, H.; Klene, M.; Li, X.; Knox, J. E.; Hratchian, H. P.; Cross, J. B.; Bakken, V.; Adamo, C.; Jaramillo, J.; Gomperts, R.; Stratmann, R. E.; Yazyev, O.; Austin, A. J.; Cammi, R.; Pomelli, C.; Ochterski, J. W.; Ayala, P. Y.; Morokuma, K.; Voth, G. A.; Salvador, P.; Dannenberg, J. J.; Zakrzewski, V. G.; Dapprich, S.; Daniels, A. D.; Strain, M. C.; Farkas, O.; Malick, D. K.; Rabuck, A. D.; Raghavachari, K.; Foresman, J. B.; Ortiz, J. V.; Cui, Q.; Baboul, A. G.; Clifford, S.; Cioslowski, J.; Stefanov, B. B.; Liu, G.; Liashenko, A.; Piskorz, P.; Komaromi, I.; Martin, R. L.; Fox, D. J.; Keith, T.; Al-Laham, M. A.; Peng, C. Y.; Nanayakkara, A.; Challacombe, M.; Gill, P. M. W.; Johnson, B.; Chen, W.; Wong, M. W.; Gonzalez, C.; Pople, J. A. *Gaussian 03*, revision B.05; Gaussian, Inc.: Pittsburgh, PA, 2003.
(41) Ottonelli, M.; Musso, G.; Comoretto, D.; Dellepiane, G. *Synth. Met.* **2001**, *124*, 253−255.
(42) Tsuzuki, S.; Honda, K.; Uchimaru, T.; Mikami, M.; Tanabe, K. *J. Am. Chem. Soc.* **2002**, *124*, 104−112.
(43) Sinnokrot, M. O.; Valeev, E. F.; Sherrill, C. D. *J. Am. Chem. Soc.* **2002**, *124*, 10887−10893.
(44) Boys, S. F.; Bernardi, F. *Mol. Phys.* **1970**, *19*, 553−566.
(45) van Duijneveldt, F. B.; van Duijneveldt-van de Rijdt, J. G. C. M.; van Lenthe, J. H. *Chem. Rev.* **1994**, *94*, 1873−1885.